



The *tert*-butoxyl radical mediated hydrogen atom transfer reactions of the Parkinsonian proneurotoxin 1-methyl-4-phenyl-1,2,3,6-tetrahydropyridine and selected tertiary amines

N. Kamrudin Suleman^{a,*}, Joey Flores^a, James M. Tanko^b, Emre Mehmet Isin^{b,†}, Neal Castagnoli Jr.^{b,c}

^a Division of Natural Sciences, University of Guam, University Drive, Mangilao, GU 96923, USA

^b Department of Chemistry, Virginia Polytechnic and State University, Blacksburg, VA 24061, USA

^c The Edward Via College of Osteopathic Medicine, Blacksburg, VA 24061, USA

ARTICLE INFO

Article history:

Received 14 June 2008

Revised 25 July 2008

Accepted 4 August 2008

Available online 7 August 2008

Keywords:

tert-Butoxyl

MPTP

Hydrogen atom transfer reactions

Regioselectivity

ABSTRACT

Previous studies have shown that the hydrogen atom transfer (HAT) reactions of *tert*-butoxyl radical from the Parkinsonian proneurotoxin 1-methyl-4-phenyl-1,2,3,6-tetrahydropyridine (MPTP) occur with low selectivity at the allylic and non-allylic α -C–H positions. In this paper, we report a more comprehensive regiochemical study on the reactivity of the *tert*-butoxyl radical as well as on the associated primary kinetic deuterium isotope effects for the various hydrogen atom abstractions of MPTP. In addition, the results of a computational study to estimate the various C–H bond dissociation energies of MPTP are presented. The results of the present study show the allylic/non-allylic selectivity is approximately 73:21. The behavior of the *tert*-butoxyl radical mediated oxidation of MPTP contrasts with this reaction as catalyzed by monoamine oxidase B (MAO-B) that occurs selectively at the allylic α -carbon. These observations lead to the conclusion that the *tert*-butoxyl radical is not a good chemical model for the MAO-B-catalyzed bioactivation of MPTP.

© 2008 Elsevier Ltd. All rights reserved.

1. Introduction

Parkinson's disease (PD) involves the progressive degeneration of nerve cells in the upper part of the brain stem known as the substantia nigra pars compacta. The reduced number of functioning nigrostriatal neurons results in diminished levels of the neurotransmitter dopamine and the associated clinical symptoms of PD in humans.^{1,2}

The western Pacific island of Guam suffers from an extraordinarily high incidence of several degenerative diseases of the central nervous system, including PD, dementia, a combination of PD and dementia (parkinsonism-dementia complex, PDC), and amyotrophic lateral sclerosis (ALS).³ In the mid-1950s, the incidence of ALS on Guam was estimated to be 50–100 times higher than the rest of the world.⁴ Although the high incidence of ALS appears to be declining, the present day occurrence of Guam PDC continues to be disproportionately high.⁵ The precise etiology of worldwide (sporadic) PD remains unknown. In the case of the Guamanian degenerative diseases, studies indicate that the etiology may

involve environmental or a combination of genetic and environmental factors.^{6–8}

Monoamine oxidases A and B (MAO-A, MAO-B) are flavoproteins that catalyze the α -carbon oxidation of neurotransmitters and other endogenous and xenobiotic amines.⁹ Both MAO-A and MAO-B are important drug targets for the treatment of neurological disorders.¹⁰ For example, in PD patients, dopamine deficiency may be further exacerbated by the neurotransmitter-degrading action of MAO-A and MAO-B.¹¹ Thus, one of the present strategies for the treatment of PD includes the administration of MAO-B inhibitors.¹² The MAO-B inhibitors provide symptomatic relief by reducing the enzyme's activity and attenuating further destruction of the already depleted dopamine levels in PD patients.¹³

For over two decades, intense efforts have been made to elucidate the catalytic mechanism of MAO.⁹ This research has been fueled in part by the expectation that a detailed understanding of the mechanism for MAO catalysis will play a key role in the design and development of new therapies and treatments for neurological disorders. Several mechanisms for MAO catalysis have been postulated as a result of these mechanistic studies.¹⁴ Initially, the available experimental evidence supported either a direct hydrogen atom transfer (HAT)¹⁵ process or a mechanism involving single electron transfer (SET).⁹ The results of more recent X-ray studies have been interpreted as evidence for a polar, nucleophilic mechanism.¹⁶ A catalytic pathway involving free radicals and radical ions

* Corresponding author. Tel.: +1 671 735 2834; fax: +1 671 734 1299.

E-mail address: nsuleman@ugam.uog.edu (N.K. Suleman).

[†] Present address: Department of DMPK and Bioanalytical Chemistry, AstraZeneca R&D Mölndal, S-431 83 Mölndal, Sweden.

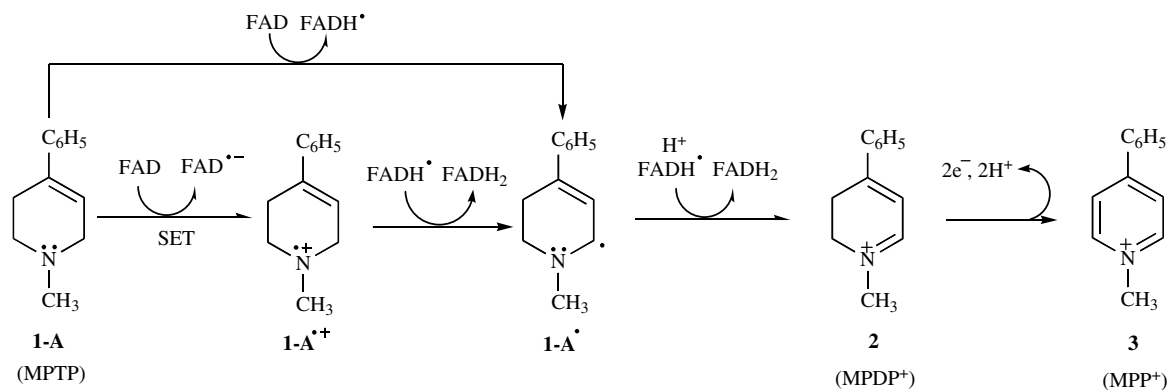


Figure 1. The HAT and SET mechanisms postulated for the MAO-B-catalyzed oxidation of MPTP to MPDP⁺.

also has received new experimental support.¹⁷ Thus, the issue of the detailed mechanism of MAO catalysis continues to be controversial.¹⁸

The overall goal of our investigations was to employ solution phase chemical modeling studies[‡] to gain a better understanding of the HAT process that had been postulated to operate in the MAO-catalyzed oxidation of 1-methyl-4-phenyl-1,2,3,6-tetrahydropyridine (MPTP). MPTP is a cyclic tertiary allylamine and a unique environmental toxin in that systemic exposure to this compound leads to the irreversible loss of nigrostriatal neurons and the symptoms of Parkinson's disease in humans.¹⁹ Previous studies have established that MPTP is oxidized in a reaction catalyzed by MAO-B to form the unstable dihydropyridinium intermediate MPDP⁺.²⁰ Subsequent non-enzymatic processes ultimately produce the Parkinsonian neurotoxin MPP⁺. Figure 1 depicts the HAT and SET mechanisms proposed for the MAO-B-catalyzed transformation of MPTP to MPDP⁺.

The HAT mechanism was considered to be a good candidate for the oxidation of MPTP for two reasons. Firstly, our studies revealed that the allylic C–H bond, α - to the nitrogen, is very weak, in the range of 75–80 kcal/mol (vide infra). The weakness of the α -allylic C–H renders this hydrogen atom especially susceptible to homolytic abstraction. Secondly, the alternative, most widely accepted non-radical mechanism for MAO catalysis is a polar nucleophilic pathway which is unlikely to operate for substrates such as MPTP. The polar mechanism, shown in Figure 2, is known to be sensitive to steric effects and, whereas primary and secondary amines may add to the flavin, this process is expected to be sterically unfavorable and therefore much less likely for tertiary amines such as MPTP.

An important aspect of chemical modeling studies is the selection of a chemical species of appropriate structure and reactivity to serve as the model. The *tert*-butoxyl radical (^tBuO[•]) is a prototypical hydrogen-abstracting radical that has been employed in numerous modeling studies that require a reactive oxygen-based free radical. This radical, for example, has been used in mechanistic studies to mimic oxidation processes in lubricants²¹ and in living systems,²² as well as in the atmosphere.²³ Specific instances where ^tBuO[•] has been used to study mechanisms of enzyme-catalyzed reactions include cytochrome P450,²⁴ methane monooxygenase,²⁵ and monoamine oxidase.²⁶ Given the widespread acceptance of ^tBuO[•]

as a model for hydrogen abstraction reactions, we elected to use this species in our studies.

In our initial modeling studies, we utilized the well-established laser flash photolysis (LFP) method to study some basic HAT reactions of MPTP with ^tBuO[•].²⁷ These studies revealed some interesting results, including the direct observation of a transient species with a λ_{max} at 385 nm. We had originally ascribed this absorption to the HAT-generated radical at the α -allylic (C₆–H) position with the proposed regioselectivity being based on the weakness of this bond. Subsequently, we became uncertain of this assignment when deuterium isotope studies indicated that ^tBuO[•] also produces other MPTP-derived radicals by abstracting hydrogen atoms from the C-2 and possibly from the *N*-methyl group in MPTP. Prompted by the unexpected deuterium isotope effects in MPTP, we undertook a thorough study of the selectivity patterns of ^tBuO[•] with a wide variety of tertiary amines and other substrates and provided a detailed analysis of the general reaction dynamics (reaction rates and activation parameters) for hydrogen abstraction reactions of ^tBuO[•].²⁸ Although these studies significantly improved our understanding of HAT processes involving ^tBuO[•], three important issues pertaining to MPTP/^tBuO[•] reactivity remained unresolved. Firstly, our knowledge of all the relevant bond dissociation energies in MPTP was incomplete. Therefore, using MO theory, we conducted studies to estimate the pertinent C–H bond dissociation energies in MPTP. Secondly, we sought to establish the identity of transient species with λ_{max} 385 nm. Thirdly, we lacked a detailed understanding of the regioselectivity of attack by ^tBuO[•] on MPTP. Consequently, in this investigation, we significantly expanded the scope of our original studies by mapping out the regioselectivity of attack by ^tBuO[•] on MPTP, as well as by determining the primary kinetic isotope effects at each position using two additional deuterium substituted MPTP derivatives and three other model compounds. In the present article, we report the results of these studies. Additionally, the findings and implications of our combined investigations are discussed in the context of ^tBuO[•] and its utility as a model for HAT processes in MAO catalysis.

2. Results and discussion

2.1. Estimation of C–H bond dissociation energies in MPTP

Values of the C–H bond dissociation energies for MPTP were estimated using density functional theory following a procedure described previously. Briefly, geometry optimizations at the B3LYP/6-31G* level followed by single point energy calculations [B3LYP/CC-PVTZ(-F)] were performed on MPTP and its corresponding free radicals to estimate the corresponding differences in energies (ΔE). Using this ΔE , the unknown C–H BDE was estimated

[‡] In the context of such studies, 'chemical modeling' implies fully characterizing the reactivity of a substrate toward the general type of chemical species that is suspected to operate in the enzymatic system. If the chemical model exhibits a comparable pattern of reactivity to the enzymatic reaction, then this could be construed as evidence that the enzyme contains a similar reactive intermediate to the model employed.

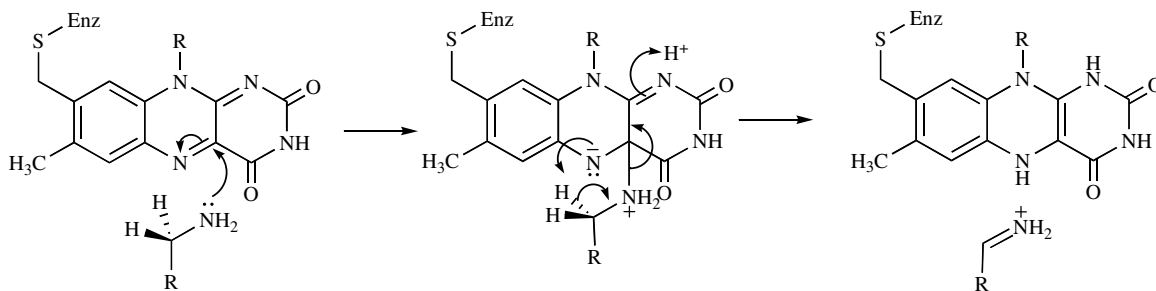


Figure 2. The polar nucleophilic mechanism postulated for MAO catalysis.¹⁶

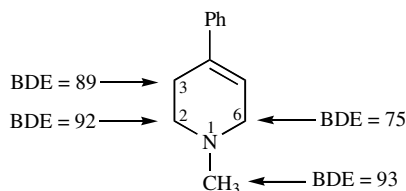


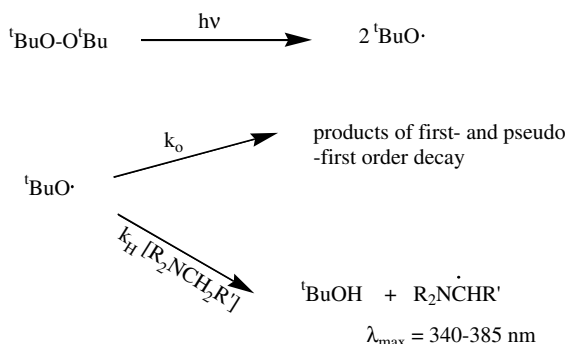
Figure 3. Estimates of the bond dissociation energies (kcal/mol) in MPTP.

from a calibration curve (plot of BDE vs ΔE based on 17 compounds with known C–H BDE's ranging from 81 to 132 kcal/mol). The results of this analysis are summarized in Figure 3.

2.2. Determination of absolute rate constants for hydrogen atom abstraction by $^t\text{BuO}^\bullet$ from MPTP

The absolute rate constants for hydrogen atom abstraction by $^t\text{BuO}^\bullet$ from MPTP and its deuterated derivatives were measured using the LFP method developed by Scaiano et al.^{29,30} In brief, this approach involves directing a short laser pulse (4–6 ns) at a solution of the aminyl substrate and di-*tert*-butyl peroxide. The resulting $^t\text{BuO}^\bullet$, formed by photolysis of the peroxide, decays through beta-scission [$(\text{CH}_3)_3\text{CO}^\bullet \rightarrow (\text{CH}_3)_2\text{C}=\text{O} + \text{CH}_3^\bullet$] and H-abstraction from solvent (first order and pseudo-first order processes, respectively) as well as through reactions with the aminyl substrate (a second order process) (Scheme 1).

In the case of MPTP (and all of its deuterated derivatives), the LFP experiments and subsequent kinetic analyses were made simple by the fact that the radical species derived from the MPTP showed a strong transient absorption band at 385 nm (Fig. 4). Hence, following the laser pulse, the growth of the MPTP-derived radical was conveniently measured by directly monitoring the change in absorption of its UV band (inset in Fig. 4).



Scheme 1. LFP of di-*tert*-butyl peroxide in the presence of tertiary amines. The $^t\text{BuO}^\bullet$ does not absorb significantly >300 nm.

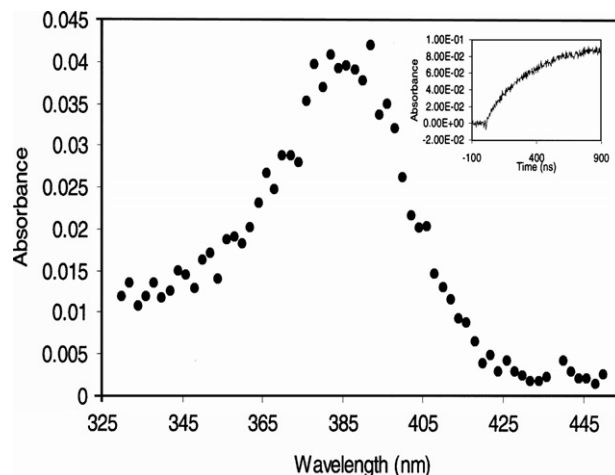


Figure 4. Transient UV spectrum of the radical species derived from the reaction of MPTP and *tert*-butoxyl. (Inset) Change in the UV absorption of the sample versus time after laser photolysis (monitored at 385 nm).

A standard pseudo-first order kinetic treatment of the data shown in Figure 4 (inset) yields the observed rate constant k_{obs} , representing the sum of all the rate constants for reactions involving $^t\text{BuO}^\bullet$. Data from multiple laser shots of each sample containing the aminyl substrate and di-*tert*-butylperoxide were used to compute an average value for k_{obs} . The experiments were performed at 8–10 different amine concentrations, with the amine concentration typically varying by at least one order of magnitude. This was done to obtain an accurate value for k_{obs} and to ensure the validity of the pseudo-first order kinetics approximation over the entire amine concentration range. Under such conditions, a linear variation between k_{obs} and [Amine] was observed and the value of the absolute rate constant for the abstraction reaction, k_{H} , was determined from the slope of the linear function described by the expression: $k_{\text{obs}} = k_0 + k_{\text{H}}[\text{Amine}]$.

The bimolecular rate constant (k_{H}) for the reaction of MPTP and $^t\text{BuO}^\bullet$ was found to be $2.27 \times 10^8 \text{ M}^{-1} \text{ s}^{-1}$. This value is similar to those obtained in previous studies for 3° amines such as triethylamine ($1.8 \times 10^8 \text{ M}^{-1} \text{ s}^{-1}$) and *N,N*-diethylaniline ($1.3 \times 10^8 \text{ M}^{-1} \text{ s}^{-1}$).³⁰ In the latter two instances, the HAT process was found to occur primarily at the C–H located adjacent to the N, producing α -aminyl radicals. In the case of MPTP, the α -allylic (C-6) position was expected to be the most likely candidate for H-abstraction (vide infra).

2.3. Kinetic deuterium isotope effect (KDIE) studies

Detailed KDIE studies on the MAO-B-catalyzed oxidation of deuterated MPTP analogs had clearly established the regioselectivity of the reaction to be at the allylic (C-6) position on MPTP.³¹ This

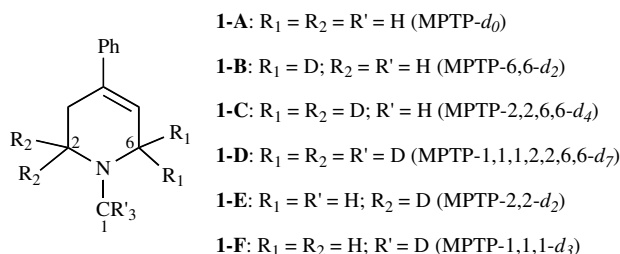


Figure 5. MPTP and deuterated analogs pertinent to this study.

Table 1

Absolute rate constants and kinetic deuterium isotope effects (KDIE) for the reaction of MPTP derivatives and *tert*-butoxyl at 25 °C in benzene

Compound	$k_H \times 10^{-8} \text{ (M}^{-1} \text{ s}^{-1}\text{)}$	k_H/k_D
MPTP (1-A)	2.27 (± 0.06)	—
MPTP-6,6- d_2 (1-B)	1.60 (± 0.14)	1.41 (± 0.13) ^a
MPTP-2,2,6,6- d_4 (1-C)	1.21 (± 0.20)	1.30 (± 0.25) ^b
MPTP-1,1,1,2,2,6,6- d_7 (1-D)	1.07 (± 0.15)	1.13 (± 0.25) ^c
MPTP-2,2- d_2 (1-E)	2.02 (± 0.02)	1.13 (± 0.03) ^d
MPTP-1,1,1- d_3 (1-F)	2.30 (± 0.10)	0.98 (± 0.07) ^e

Uncertainties in the last reported digits are in parentheses.

^a d_2 versus d_0 .

^b d_2 versus d_4 .

^c d_4 versus d_7 .

^d d_2 versus d_0 .

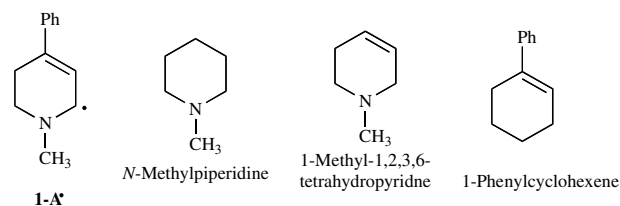
^e d_3 versus d_0 .

conclusion was based on the observation of a significant KDIE effect on position 6, but no KDIE at positions 1 or 2 of MPTP. In order to provide a basis for comparing the enzymatic and chemical oxidations of MPTP, we undertook a comprehensive KDIE study to delineate the regioselectivity of attack by ^tBuO[•] on MPTP (Fig. 5). Table 1 summarizes the completed KDIE study using the LFP method for MPTP/^tBuO[•].

Table 1 shows that the magnitudes of $k_{H/D}$ observed for the HAT reaction between MPTP/^tBuO[•] are small. These results are comparable to those previously reported for ^tBuO[•] and (CH₃)₃N/(CD₃)₃N in which $k_{H/D}$ was reported to be 1.4.³⁰ In both of these instances, the small magnitude of the isotope effect can be explained as follows. The strength of the O–H bond in ^tBuOH is 105 kcal/mol while the α -C–H bonds of most amines lay in the range of approximately 80–95 kcal/mol. Thus, the HAT reactions between 3° amines and ^tBuO[•] are exothermic by at least 10 kcal/mol.³² In such highly exothermic cases, the reactions are generally characterized by early transition states in which there is relatively little bond breaking, thus producing a nominal effect from substitution by deuterium.

In terms of regioselectivity, the additional KDIE studies confirmed our earlier findings that the abstraction of H atoms by *tert*-butoxyl from MPTP occurs at both the C-6 and C-2 α -methylene positions and, possibly, at the (C-1)- α -methyl as well.[§] Although ^tBuO[•] has long been known to be a highly reactive hydrogen-abstracting radical, this was nonetheless an unexpected finding. Indeed, given the presence of the significantly weakened α -allylic C-6 hydrogen bond in MPTP, substantially greater allylic to non-allylic selectivity was expected. Further studies revealed that the lack of selectivity in the reactions between 3° amines and ^tBuO[•] is quite general. A quintessential example of this is the observation that ^tBuO[•] reacts with triallylamine at a slightly lower

[§] The small intrinsic H/D isotope effects, coupled with the relatively large errors associated with the LFP method ($\pm 10\%$), prevent us from drawing a definite conclusion regarding abstraction from the α -methyl position.



Scheme 2. Model compounds used in this study to ascertain the UV/vis features of MPTP-derived radical 1-A'.

rate constant than with triethylamine, despite the fact that the C–H BDE for the latter is greater by 8.1 kcal/mol.^{**}

The MPTP/^tBuO[•] results are in sharp contrast with the conclusions reached regarding the MAO-B-catalyzed oxidation of MPTP (vide supra). However, the precise implications of the disparate behavior of our model system and the enzymatic reaction are not entirely clear. Assuming that a HAT mechanism is operating in the enzymatic reaction, one possible conclusion is that the hydrogen atom abstracting species in the enzyme possesses much lower reactivity and hence a much higher intrinsic selectivity than ^tBuO[•]. An alternate interpretation is that the high regioselectivity observed in the MAO-B-catalyzed oxidation of MPTP is a consequence of the favorable spatial relationship of the substrate with respect to the abstracting radical in the active site of the enzyme. Based on our experimental results, we are not able to evaluate the likelihood of either of the above interpretations.

2.4. Chromophore studies related to MPTP-derived radicals

The transient absorption shown in Figure 4 was initially ascribed to the MPTP-derived radical 1-A', consistent with earlier reports for the reaction of ^tBuO[•] with triallyl amine ($\lambda_{\max} = 430 \text{ nm}$).³³ However, our KDIE results subsequently led us to question this assignment, since it was clear that hydrogen atom abstraction was not taking place exclusively at the α -allylic position. Model studies using the compounds depicted in Scheme 2 were thus undertaken to help establish the identity of species responsible for the strong absorption ($\lambda_{\max} = 385 \text{ nm}$). Using the laser flash photolysis (LFP) technique, it was shown that the radicals produced from the reaction of ^tBuO[•] with *N*-methylpiperidine showed a weak absorbance with a $\lambda_{\max} < 340 \text{ nm}$. A second model compound, 1-methyl-1,2,3,6-tetrahydropyridine, gave a similar result. A third compound, 1-phenylcyclohexene, showed no perceptible absorption above 340 nm. Collectively, these data support the hypothesis that the aforementioned 385 nm chromophore arises from MPTP that has undergone hydrogen atom abstraction at the allylic (C-6) position, α - to the nitrogen atom and in conjugation with the styrenyl system.

2.5. Regioselectivity studies

In order to confirm the KDIE studies and help establish the regioselectivity of ^tBuO[•] attack on MPTP, studies were carried out to determine the overall rate constants for the reaction of ^tBuO[•] with the model compounds mentioned in 2.4. LFP yielded the following rate constants for reaction with ^tBuO[•] at 25 °C: *N*-methylpiperidine ($1.0 \times 10^8 \text{ M}^{-1} \text{ s}^{-1}$), 1-methyl-1,2,3,6-tetrahydropyridine ($1.6 \times 10^8 \text{ M}^{-1} \text{ s}^{-1}$), and 1-phenylcyclohexene ($1.6 \times 10^7 \text{ M}^{-1} \text{ s}^{-1}$). Since 1-phenylcyclohexene showed no perceptible absorption above 340 nm, the rate constant for this compound was determined using the 'probe' method, as discussed in Section 4. The value for

^{**} The 3° amine/^tBuO[•] results have since been explained on the basis of entropy control in these reactions. A detailed discussion on this topic can be found in Ref. 28.

N-methylpiperidine was consistent with expectations based on our previous studies involving 3° amines. The rate constant for 1-methyl-1,2,3,6-tetrahydropyridine compares very favorably to that of *N*-methylpiperidine and clearly indicates that further conjugation (i.e., with a vinyl group in this case) does not cause a significant enhancement of the overall rate constant. The model study with 1-phenylcyclohexene suggests that H-abstraction from C-3 contributes <10% to the total rate constant for MPTP ($1.6 \times 10^7 \text{ M}^{-1} \text{ s}^{-1}$ vs $2.3 \times 10^8 \text{ M}^{-1} \text{ s}^{-1}$). With the stated error limits of $\pm 10\%$, the LFP method is not sensitive enough to detect H-abstraction from C-3, and it is assumed to be essentially zero. Thus for compound 1-A (MPTP), the observed rate constant k_A is the sum of the rate constants for H-abstraction from C-2, C-6, and the *N*-methyl group:

$$k_A = k_2 + k_6 + k_{\text{Me}} = 2.27(\pm 0.06) \times 10^8 \text{ M}^{-1} \text{ s}^{-1} \quad (1)$$

For the remaining compounds listed in Table 1 (letting d = the deuterium labeled positions):

$$k_B = k_2 + k_{6d} + k_{\text{Me}} = 1.60(\pm 0.14) \times 10^8 \text{ M}^{-1} \text{ s}^{-1} \quad (2)$$

$$k_C = k_{2d} + k_{6d} + k_{\text{Me}} = 2.02(\pm 0.02) \times 10^8 \text{ M}^{-1} \text{ s}^{-1} \quad (3)$$

$$k_D = k_{2d} + k_{6d} + k_{\text{Me}} = 1.21(\pm 0.20) \times 10^8 \text{ M}^{-1} \text{ s}^{-1} \quad (4)$$

$$k_E = k_{2d} + k_{6d} + k_{\text{Me-d}} = 1.07(\pm 0.15) \times 10^8 \text{ M}^{-1} \text{ s}^{-1} \quad (5)$$

$$k_F = k_2 + k_6 + k_{\text{Me-d}} = 2.30(\pm 0.10) \times 10^8 \text{ M}^{-1} \text{ s}^{-1} \quad (6)$$

Subtracting Eq. (5) from Eq. (4):

$$k_{\text{Me}} - k_{\text{Me-d}} = k_D - k_E = 0.14(\pm 0.04) \times 10^8 \text{ M}^{-1} \text{ s}^{-1} \quad (7)$$

Eq. (4) from Eq. (2):

$$k_2 - k_{2d} = k_B - k_D = 0.39(\pm 0.10) \times 10^8 \text{ M}^{-1} \text{ s}^{-1} \quad (8)$$

And Eq. (4) from Eq. (3):

$$k_6 - k_{6d} = k_C - k_D = 0.81(\pm 0.20) \times 10^8 \text{ M}^{-1} \text{ s}^{-1} \quad (9)$$

From the experimental finding that $k_A = k_F$ (within experimental error), it can be reasonably surmised that the rate constant for *N*-methylpiperidine represents H-abstraction mainly from the α -*N* methylene carbon atoms, and that this rate constant represents a good model for C-2 of MPTP. This leads to $k_2 = 5.0 (\pm 0.10) \times 10^7 \text{ M}^{-1} \text{ s}^{-1}$ (after a statistical correction—two vs four equivalent hydrogens). Additionally, the fact that $k_A = k_F$ must mean that k_{Me} , $k_{\text{Me-d}} \ll k_2$, k_6 . Using Eq. (1), assuming k_{Me} is small, leads to $k_6 = 1.77 (\pm 0.06) \times 10^8 \text{ M}^{-1} \text{ s}^{-1}$. Solving for the remaining unknowns results in

$$k_{2d} = 1.1(\pm 0.3) \times 10^7 \text{ M}^{-1} \text{ s}^{-1}$$

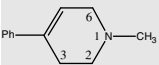
$$k_{6d} = 9.6(\pm 2.0) \times 10^7 \text{ M}^{-1} \text{ s}^{-1}$$

$$k_{\text{Me}} = 1.4(\pm 0.4) \times 10^7 \text{ M}^{-1} \text{ s}^{-1}$$

$$k_{\text{Me-d}} < 3 \times 10^6 \text{ M}^{-1} \text{ s}^{-1} \text{ (estimate, too low to detect)}$$

Table 2

Estimates of the % attack by $^t\text{BuO}^\bullet$, individual kinetic isotope effects, and bond dissociation energies in MPTP

Position in MPTP	% Attack by $^t\text{BuO}^\bullet$	Individual isotope effect	Bond dissociation energy (kcal/mol)
			
1 (–CH ₃)	<6	4.7	93
2	21	4.5	92
3	<10	—	89
6	73	1.84	75

The above data enable us to provide an estimate for the %-abstraction at each position in MPTP, as well as the individual isotope effects shown in Table 2 (also included are the calculated BDEs (kcal/mol) discussed in Section 2.1).

The regioselectivity studies and quantitative treatment of the kinetic data reveal several important points. Firstly, a substantial fraction (approximately 73%) of the H-abstraction occurs at C-6. This finding is consistent with the fact that C-6 has the weakest C–H bond in MPTP. In addition, the low isotope effect for C-6 (1.84) indicates an early transition state for the C–H abstraction. This observation is consistent with a highly exothermic reaction, prompted presumably by the very weak C–H bond. Secondly, our studies indicate that a smaller but nonetheless significant fraction (21%) of H-abstraction occurs from C-2. The smaller percentage of C–H abstraction and larger isotope effect for C-2 reflect the stronger C–H bond at C-2. Thirdly, H-abstraction at the *N*-methyl position in MPTP could not be clearly detected beyond the error limits of our experiments. Our data indicate that, while this process could be occurring, it constitutes a very small fraction (<6%) of the total abstraction in MPTP. Finally, our results show that the allylic CH₂ in MPTP (C-6) is only 3.5 times more reactive toward $^t\text{BuO}^\bullet$ than the non-allylic CH₂ (C-2). This represents a very low level of selectivity given the substantial differences in BDEs of the respective C–H bonds.

3. Conclusions

The studies reported in this paper have significantly improved our understanding of the reactions of $^t\text{BuO}^\bullet$ with MPTP, an important Parkinsonian proneurotoxin. The contributions of the present studies are threefold. We have determined the C–H bond dissociation energies in MPTP, identified the spectroscopic transient radical produced in the reactions of $^t\text{BuO}^\bullet$ with MPTP, and delineated the regioselectivity of attack by $^t\text{BuO}^\bullet$ on the various C–H bonds in MPTP.

An important additional finding of our combined studies is that, in some instances (such as MPTP), $^t\text{BuO}^\bullet$ exhibits low levels of regioselectivity. This shortcoming of $^t\text{BuO}^\bullet$ is most readily apparent in reactions with reactive substrates containing weak C–H bonds (<92 kcal/mol), such as those found in unsymmetrical 3° amines. We attribute the low levels of selectivity in the above cases to the fact that these reactions are entropy-controlled. With reactive substrates containing weak C–H bonds, the enthalpy of activation (ΔH^\ddagger) is low, and, as a consequence, $T\Delta S^\ddagger$ is the main contributor to the free energy of activation (ΔG^\ddagger). In short, the reaction barrier is governed more by issues of orientation and trajectory, than by the strength of the C–H bond being broken.

We conclude therefore that $^t\text{BuO}^\bullet$ is not an appropriate free radical with which to test the HAT mechanism that has been postulated for the MAO-catalyzed oxidation of MPTP. Future studies plan to explore the potential utility of less reactive (and presumably more selective) oxygen-based free radicals such as phenoxyl³⁴ as models for the α -C–H bond cleavage in the MAO-catalyzed oxidation of MPTP and amines in general.

4. Experimental

4.1. Materials

All chemicals and solvents were of the highest grade available. The di-*tert*-butyl peroxide was passed through a column of activated basic alumina immediately prior to use. The *N*-methylpiperidine, *N,N*-dimethylaniline, and 1-phenylcyclohexene were distilled at reduced pressure and stored under dry nitrogen at -5°C . The benzene and 1-methyl-1,2,3,6-tetrahydropyridine were used as received. MPTP and all the deuterated MPTP derivatives used in this study

were synthesized according to literature procedures.³¹ The 1-methyl-1,2,3,6-tetrahydropyridine, as well as all the MPTP compounds were stored either as their hydrochloride or oxalate salts. The aforementioned salts were treated with aqueous potassium carbonate to generate the free amine just prior to LFP. *Caution:* MPTP is a known nigrostriatal neurotoxin and should be handled using disposable gloves in a properly ventilated hood. Detailed procedures for the safe handling of MPTP have been reported.³⁵

4.2. Instrumentation

Steady-state UV–visible spectra were recorded on a Hewlett-Packard 8452A Spectrometer. Unless otherwise noted, LFP experiments were conducted on an Applied Photophysics LKS.60 spectrometer using the third harmonic (355 nm) of a Continuum Surelite I-10 Nd:YAG laser. The pulse duration was typically 4–6 ns. Transient signals were monitored by an HP Infinium digital oscilloscope and analyzed with the Applied Photophysics SpectraKinetic Workstation software package (v.4.59). For MPTP-2,2-d₂, the LFP experiments were carried out using a Lambda Physik Lextra 50 excimer laser (XeCl, 308 nm; <180 mJ/pulse; 10 ns pulses) and a Lambda Physik LPD 3002 pumped-dye laser (*p*-terphenyl dye for 343 nm; <10 mJ/pulse; 7 ns pulses). The excitation pulses were attenuated, when necessary, using neutral density filters. Transient absorptions were monitored at right angles to the excitation. A pulsed Oriel 150 W xenon lamp (Model 66007) was used as the monitoring beam. The analyzing beam was collected and focused on the entrance slit (2 nm) of an Instrument S.A. H-20 monochromator. A Hamamatsu R-446 photomultiplier tube (PMT) in a custom housing (Products for Research) was attached to the exit slit of the monochromator. A computer-controlled Stanford Research Systems high voltage power supply (Model PS310) was used with the PMT. The signals from the PMT were digitized using a Tektronix TDS 620 oscilloscope and transferred to a PC, via a GPIB interface, for data storage and processing. A Quantum Composer pulse generator (Model 9318) provided TTL trigger pulses to control the timing for the laser, lamp, and oscilloscope. Appropriate long pass filters were placed on either side of the sample to prevent photolysis by the analyzing light.

4.3. Laser flash photolysis (LFP)

All LFP samples were prepared according to a standardized protocol in which the free amine was added to a deoxygenated solution of benzene containing 7.5–20% di-*tert*-butyl peroxide. The mixture was then transferred to multiple quartz cuvettes and the contents were deoxygenated further with a gentle stream of nitrogen for 20 min under subdued light. A UV–vis analysis was performed for each sample to ensure that the di-*tert*-butyl peroxide was the only absorbing species at the excitation wavelength. Each cuvette was equilibrated at 25 °C for ten minutes in the thermostated cell holder prior to LFP. For all LFP experiments, the laser power was carefully curtailed to eliminate the contributions of radical–radical processes to the observed rate constants (i.e., the variation of the observed rate constant as a function of laser power was determined for each experiment. Only those data which were collected in the power-independent regime were deemed acceptable). The experiments were performed at between eight to ten different amine concentrations, with the amine concentration typically varying by at least one order of magnitude. The LFP experiments involving 1-phenylcyclohexene were slightly modified since this compound produced no perceptible signal above 340 nm when irradiated in the presence of di-*tert*-butyl peroxide. These experiments were therefore carried out in the presence of a fixed amount (typically 0.05 M) of *N,N*-dimethylaniline, used as a spectroscopic probe, with the signal analyzed at 340 nm.

Acknowledgments

The authors gratefully acknowledge generous support of this research by the following: The Harvey W. Peters Research Center for Parkinson's Disease and Disorders of the Central Nervous System in Blacksburg, Virginia, NIH/MBRS/SCORE Grant # 53H 720454 and NIH/MBRS/RISE Grant # 53H 620454 to the University of Guam, and the National Science Foundation (CHE-0548129, Virginia Tech). Special thanks to Professor J. Dinnocenzo for allowing us the use of the LFP apparatus at The Center for Photoinduced Charge Transfer, University of Rochester.

References and notes

- Chung, K. K.; Dawson, V. L.; Dawson, T. M. *J. Neurol.* **2003**, 250(Suppl. 3), III/15–III/24.
- Lozano, A. M.; Lang, A. E.; Hutchison, W. D.; Dostrovsky, J. O. *Curr. Opin. Neurobiol.* **1998**, 8, 783–790.
- Ahlskog, J. E.; Petersen, R. C.; Waring, S. C.; Esteban-Santillan, C.; Craig, U.-K.; Maraganore, D. M.; Lennon, V. A.; Kurland, L. T. *Neurology* **1997**, 48(5), 1356–1362.
- Plato, C. C.; Galasko, D.; Garruto, R. M.; Plato, M.; Gamst, A.; Craig, U.-K.; Torres, J. M.; Wiederholt, W. *Neurology* **2002**, 58(5), 765–773.
- Galasko, D.; Salmon, D. P.; Craig, U.-K.; Thal, L. J.; Schellenberg, G.; Wiederholt, W. *Neurology* **2002**, 58(1), 90–97.
- Sebeo, J.; Hof, P. R.; Perl, D. P. *Acta Neuropathol.* **2004**, 107(6), 497–503.
- Khabazian, I.; Bains, J. S.; Williams, D. E.; Cheung, J.; Wilson, J. M. B.; Pasqualotto, B. A.; Pelech, S. L.; Andersen, R. J.; Wang, Y.-T.; Liu, L.; Nagai, A.; Kim, S. U.; Craig, U.-K.; Shaw, C. A. *J. Neurochem.* **2002**, 82(3), 516–528.
- Thiruchelvam, M.; Richfield, E. K.; Goodman, B. M.; Baggs, R. M.; Cory-Slechta, D. A. *Neurotoxicology* **2002**, 23, 621–633.
- Silverman, R. B. *Acc. Chem. Res.* **1995**, 28(8), 335–342.
- Binda, C.; Newton-Vinson, P.; Hubalek, F.; Edmondson, D. E.; Mattevi, A. *Nat. Struct. Biol.* **2002**, 9(1), 22–26.
- Rinne, U. K. *J. Neural. Transm.* **1987**, 25(Suppl.), 149–155.
- Savitt, J. M.; Dawson, V. L.; Dawson, T. M. *J. Clin. Invest.* **2006**, 116, 1744–1754.
- Chrisp, P.; Mammen, G. L.; Sorkin, E. M. *Drugs Aging* **1991**, 1, 228–248.
- Mitchell, D. A.; Nikolic, D.; van Breeman, R. B.; Silverman, R. B. *Bioorg. Med. Chem. Lett.* **2001**, 11, 1757–1760.
- Edmondson, D. E. *Xenobiotica* **1995**, 25, 735–753.
- Edmondson, D. E.; Mattevi, A.; Binda, C.; Li, M.; Hubalek, F. *Curr. Med. Chem.* **2004**, 11, 1983–1993.
- Rigby, S. E.; Hynson, R. M. G.; Ramsay, R. R.; Munro, A. W.; Scrutton, N. S. *J. Biol. Chem.* **2005**(6), 4627–4631.
- Scrutton, N. S. *Nat. Prod. Rep.* **2004**, 21, 722–730.
- Langston, J. W.; Forno, L. S.; Tetrad, J.; Reeves, A. G.; Kaplan, J. A.; Karluk, D. *Ann. Neurol.* **1999**, 46(4), 598–605.
- Chiba, K.; Trevor, A. J.; Castagnoli, N., Jr. *Biochem. Biophys. Res. Commun.* **1984**(120), 574–578.
- Lindsay Smith, J. R.; Nagatomi, E.; Stead, A.; Waddington, D. J.; Beviere, S. D. *J. Chem. Soc. Perkin Trans. 2* **2000**, 1193–1198.
- Adam, W.; Marquardt, S.; Kemmer, D.; Saha-Moeller, C. R.; Schreier, P. *Org. Lett.* **2002**, 4, 225–228.
- Hudson, A.; Waterman, D.; Alberti, A. J. *J. Chem. Soc. Perkin Trans. 2* **1995**, 2091–2093.
- Karki, S. B.; Dinnocenzo, J. P.; Jones, J. P.; Korzekwa, K. R. *J. Am. Chem. Soc.* **1995**, 117(13), 3657–3664.
- Choi, S.-Y.; Eaton, P. E.; Hollenberg, P. F.; Liu, K. E.; Lippard, S. J.; Newcomb, M.; Putt, D. A.; Upadhyaya, S. P.; Xiong, Y. *J. Am. Chem. Soc.* **1996**, 118, 6547–6555.
- Franot, C.; Mabie, S.; Castagnoli, N., Jr. *Bioorg. Med. Chem.* **1998**, 6(3), 283–291.
- Tanko, J. M.; Friedline, R.; Suleman, N.; Kamrudin; Castagnoli, N., Jr. *J. Am. Chem. Soc.* **2001**, 123(24), 5808–5809.
- Finn, M.; Friedline, R.; Suleman, N.; Kamrudin; Wohl, C.; Tanko, J. M. *J. Am. Chem. Soc.* **2004**, 126(24), 7578–7584.
- Paul, H.; Small, R. D., Jr.; Scaiano, J. C. *J. Am. Chem. Soc.* **1978**, 100(14), 4520–4527.
- Griller, D.; Howard, J. A.; Marriott, P. R.; Scaiano, J. C. *J. Am. Chem. Soc.* **1981**, 103(3), 619–623.
- Ottoboni, S.; Caldera, P.; Trevor, A.; Castagnoli, N., Jr. *J. Biol. Chem.* **1989**, 264(23), 13684–13688.
- Dombrowski, G. W.; Dinnocenzo, J. P.; Farid, S.; Goodman, J. L.; Gould, I. R. *J. Org. Chem.* **1999**, 64(2), 427–431.
- Lalève, J.; Graff, B.; Allonas, X.; Fouassier, J. P. *J. Phys. Chem. A* **2007**, 111, 6991–6998.
- Foti, M.; Ingold, K. U.; Luszyk, J. *J. Am. Chem. Soc.* **1994**, 116, 9440–9447.
- Pitts, S. M.; Markey, S. P.; Murphy, D. L.; Weisz, A.; Lunn, G. Recommended practices for the safe handling of MPTP. In *MPTP-A Neurotoxin Producing a Parkinsonian Syndrome*; Academic: New York, 1986; pp 703–716.